Ga Sublattice Defects in (Ga,Mn)As: Thermodynamical and Kinetic Trends

F. Tuomisto,* K. Pennanen, and K. Saarinen
Laboratory of Physics, Helsinki University of Technology, P.O. Box 1100, 02015 HUT, Finland

J. Sadowski
Max-lab, Lund University, 22100 Lund, Sweden
Institute of Physics, Polish Academy of Sciences, 02-668 Warszawa, Poland
(Received 15 April 2004; published 30 July 2004)

We have used positron annihilation spectroscopy and infrared absorption measurements to study the Ga sublattice defects in epitaxial $Ga_{1-x}Mn_xAs$ with Mn content varying from 0% to 5%. We show that the Ga vacancy concentration decreases and As antisite concentration increases with increasing Mn content. This is in agreement with thermodynamical considerations for the electronic part of the formation energy of the Ga sublattice point defects. However, the absolute defect concentrations imply that they are determined rather by the growth kinetics than by the thermodynamical equilibrium. The As antisite concentrations in the samples are large enough to be important for compensation and magnetic properites. In addition, the Ga vacancies are likely to be involved in the diffusion and clustering of Mn at low annealing temperatures.

DOI: 10.1103/PhysRevLett.93.055505 PACS numbers: 61.72.Ji, 75.50.Pp, 78.70.Bj

The possibility to include magnetic impurities such as manganese (Mn) at high concentrations in GaAs offers good prospects of combining magnetic phenomena with high speed electronics and optoelectronics [1,2]. The ferromagnetic coupling in (Ga,Mn)As is mediated by holes [3]. Important magnetic properties, such as the Curie temperature and the saturation magnetization, have been shown to be directly related to the concentration of the holes [3–5]. Thus, the compensation of the holes is an important topic. Ingrown point defects act as compensating centers and thus have a strong effect on the magnetic properties. Their concentrations depend on the thermodynamical formation energies. However, in GaAs grown at low temperature, the growth kinetics have an influence on the defect concentrations as demonstrated before in low temperature molecular beam epitaxy (LT-MBE) grown GaAs [6–11].

In this work we investigate the thermodynamical and kinetic behavior of native point defects in LT-MBE $Ga_{1-x}Mn_xAs$. The arsenic-rich growth stoichiometry produces defects mainly in the Ga sublattice of both donor-type (As antisite As_{Ga}) and acceptor-type (Ga vacancy V_{Ga}) defects. The Ga vacancies were observed by positron annihilation spectroscopy and the As_{Ga} defects with infrared absorption spectroscopy. We show that the Ga vacancy concentration decreases with increasing Mn content, as can be expected from the thermodynamical considerations for an acceptor-type defect. However, their concentration saturates at a level that is much higher than can be estimated from thermodynamics only. The As_{Ga} concentration is shown to increase with the Mn content, in agreement with what can be expected for a donor-type defect. The concentrations of the As antisites, 10%–20% of the Mn concentration, are large enough to be important for compensation and magnetic properties. No signs of native As sublattice defects, such as the As vacancy (V_{As}) or Ga antisite (Ga_{As}), were found.

The $Ga_{1-x}Mn_xAs$ layers were grown in a Kryovak LT-MBE system dedicated to III-Mn-V magnetic semiconductors on semi-insulating (SI) Freiberger GaAs wafers at temperatures 210–240 °C; see Ref. [12] for more details. The As_2 flow was kept low during growth in order to minimize the production of As antisites. The Mn concentration in the layers was varied between 0.5% and 5% and the layer thicknesses were 0.5–1.5 μm. The hole concentrations in the as-grown layers determined by Hall measurements were about 30% of the Mn concentrations. No postgrowth annealings were performed.

The infrared absorption experiments were carried out in the transmission configuration. Three samples with $Ga_{1-x}Mn_xAs$ layer thickness 1.5 μm and Mn content of 1%, 3%, and 5% were measured. A sample cut from the substrate SI GaAs was used as a reference with the absorption coefficient of μ_{subst}. The absorption coefficient μ_{layer} of the layer was extracted from the equation $\phi_{out}(h\nu) = \phi_{in}(h\nu)\exp[-(\mu_{layer}d_{layer} + \mu_{subst}d_{subst})]$ by measuring the outcoming (ϕ_{out}) and ingoing (ϕ_{in}) light fluxes as functions of the photon energy $h\nu$, respectively. The layer and substrate thicknesses are denoted by d. The measurements were carried out using a relatively high light flux of $\phi_{in} \approx 10^{16}$ cm^{-2} s^{-1} so that the occupation of the electron states in the band gap is dominated by the optical transitions.

The positron annihilation studies were carried out using a variable energy ($E = 0$–30 keV) positron beam [13]. After implantation and rapid thermalization in the sample, the positrons can get trapped at neutral and negative vacancy defects. This can be observed as the

narrowing of the Doppler-broadened 511 keV annihilation γ peak. The measured spectra were characterized by the conventional line shape parameters S and W. S represents the fraction of positrons annihilating mainly with the valence electrons with a low longitudinal momentum component $|p_L| < 3.1 \times 10^{-3} m_0 c$ and W represents the fraction of positrons annihilating mainly with the high-momentum $(11 \times 10^{-3} m_0 c < |p_L| < 29 \times 10^{-3} m_0 c)$ core electrons. In order to study the electron-positron momentum distribution in more detail and to confirm the identity of the observed defects, we performed also coincidence measurements of the Doppler broadening with two Ge detectors. In this setup, the peak-to-background ratio can be enhanced up to 2×10^6.

Figure 1 shows the absorption coefficient of the $Ga_{1-x}Mn_xAs$ layers as a function of incoming photon energy. The steplike spectrum of the 1% layer is similar as measured many times before in Czochralski-grown bulk SI GaAs and attributed to the electron transitions from As_{Ga} defect level to the conduction and valence bands [14–17]. The main difference to SI GaAs is that here the As antisite concentration is larger by 3 orders of magnitude. The absorption coefficient μ is determined by both the concentrations of the neutral and positive antisites and the absorption cross sections of the electrons (σ_n) and holes (σ_p), respectively. Under illumination the concentrations are related through $[As^0_{Ga}] = [As^{tot}_{Ga}]\sigma_p/(\sigma_p + \sigma_n) = [As^+_{Ga}]\sigma_p/\sigma_n$ and the absorption coefficient can be written as

$$\mu = \sigma_n[As^0_{Ga}] + \sigma_p[As^+_{Ga}] = \frac{2\sigma_n\sigma_p}{\sigma_n + \sigma_p}[As^{tot}_{Ga}]. \quad (1)$$

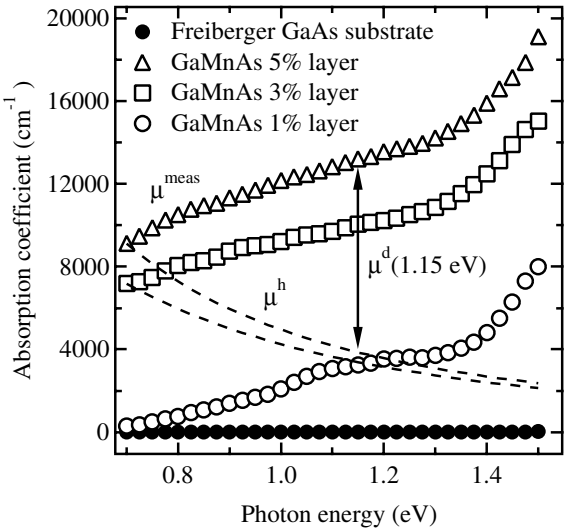

FIG. 1. The absorption coefficient of the $Ga_{1-x}Mn_xAs$ layers as a function of incoming light photon energy. The dashed lines present the estimated free carrier absorption in the layers with 3% and 5% Mn.

The value of the absorption coefficient at a certain energy is thus directly proportional to the total As antisite concentration. Conventionally, the concentration is determined from the absorption coefficient at $h\nu = 1.15$ eV. The values of σ_n and σ_p around $h\nu = 1.15$ eV have been estimated by many authors [14–17], resulting in $\sigma_0 = 2\sigma_n\sigma_p/(\sigma_n + \sigma_p) = 0.7(3) \times 10^{-16}$ cm^2.

The steplike feature is not as clearly present in the absorption coefficient of the layers with Mn content 3% and 5% as in the sample with 1% Mn. The absorption is dominated by the free carriers, consistent with the hole concentrations in the layers. The contribution of the free carriers to the absorption of light can be estimated as $\mu^h(\omega) = \epsilon_2/nc$, where ϵ_2 is the imaginary part of the dielectric function $\epsilon(\omega) = 1 - \omega_p^2/(\omega^2 + i\omega/\tau)$. Here ω_p is the hole plasma frequency that depends on the hole concentration and τ is the relaxation time that depends on the hole mobility, both of which are obtained from Hall measurements (the mobility is $\sim$20 cm^2/V s for samples with Mn content 3% or higher). The calculated absorption coefficients arising from the holes are presented in Fig. 1 for the layers with Mn content 3% and 5% [$\mu^h(\omega) \simeq 0$ for the layer with 1% of Mn]. The defect-related absorption coefficient can be estimated as $\mu^d = \mu^{meas} - \mu^h$ at photon energy $h\nu = 1.15$ eV. The results are presented in Table I. The total concentrations of the As antisites are estimated to be about 10%–20% of the Mn content.

The S and W parameters in the $Ga_{1-x}Mn_xAs$ layers were measured at room temperature as a function of the positron beam energy E (depth scan). Typical W vs E plots are presented in Fig. 2. Because of the broad positron implantation profile the data from above 15 keV are affected by annihilations in the SI GaAs substrate even in the case of the thickest (1.5 μm) layers. The stationary positron diffusion equation with a two-layer model has been fitted to the S and W vs E data (solid lines in Fig. 2) [13]. The model takes into account the positron implantation profile as well as the diffusion of the positrons to the substrate and to the surface.

The $Ga_{1-x}Mn_xAs$ layer-specific S and W parameters obtained from the data fitting are presented in Fig. 3. The results are presented as normalized to the S and W parameters of a p-type GaAs reference sample, which is free of defects detectable by positrons [18]. As can be seen

TABLE I. The As_{Ga} concentrations determined from the $Ga_{1-x}Mn_xAs$ layers. The error estimates reflect the error in the determination of the absorption coefficient.

x	μ^d (1.15 eV)	$[As^{tot}_{Ga}]$	$[As^{tot}_{Ga}]/[Mn]$
0.01	2900 cm^{-1}	$0.4(1) \times 10^{20}$ cm^{-3}	20%
0.03	6700 cm^{-1}	$1.0(2) \times 10^{20}$ cm^{-3}	17%
0.05	9400 cm^{-1}	$1.3(2) \times 10^{20}$ cm^{-3}	13%

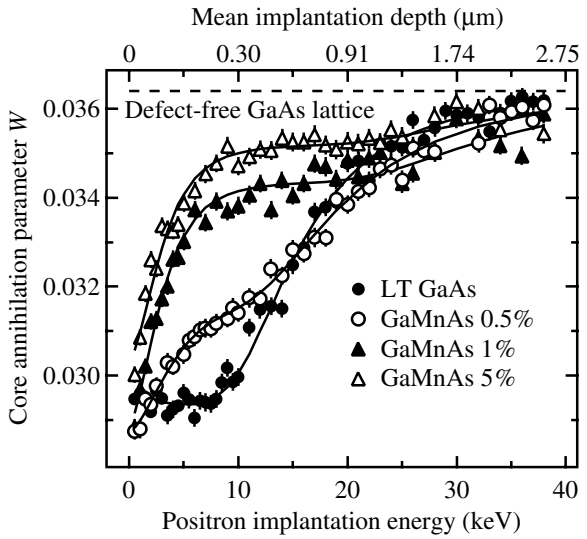

FIG. 2. The W parameter as a function of positron implantation energy measured in the $Ga_{1-x}Mn_xAs$ layers with different Mn concentrations. The solid lines are fits of the diffusion model to the data.

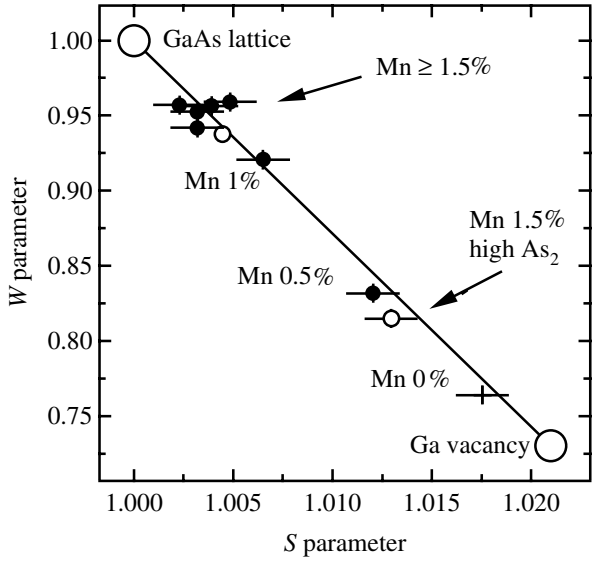

FIG. 3. The (S, W) parameters of the $Ga_{1-x}Mn_xAs$ layers with different Mn concentrations. The solid line connects the bulk and the Ga vacancy parameters. The small open circles are measured in layers where a higher As_2 flow was used during growth.

from the figure, W depends linearly on S, which indicates that the same type of vacancy defect is observed in all the layers and only the concentration varies [13]. The slope of the line is a fingerprint of a specific vacancy. Figure 3 shows the line connecting the bulk and the (S, W) parameters [1.021(3), 0.73(1)] specific to V_{Ga} [6,9]. The measured points fall on the line, thus giving evidence that the observed vacancy defect is the Ga vacancy.

Further identification of the Ga vacancy is obtained from the two-detector coincidence measurements of the Doppler broadening. The behavior of the high-momentum part of the positron-electron distribution is the same in both the LT GaAs and $Ga_{1-x}Mn_xAs$ layers, and similar as observed previously [19]. The core electron momentum distribution shows the typical signature of As $3d$ electrons [8,19], indicating directly that the vacancy is in the Ga sublattice. The isolated Ga vacancy, however, is mobile at the growth temperatures of the LT-MBE system [20]. Thus the observed Ga vacancies are most probably complexed with donor-type defects, such as As_{Ga} (as observed previously in LT GaAs [8]) or Mn_I.

In order to determine the concentrations of the Ga vacancies, we measured the S and W parameters in the layers also as a function of measurement temperature in the range 100–370 K. The decrease of the S parameter due to positron trapping at negative-ion–type defects was observed below room temperature in the layer with 0.5% of Mn, while no temperature dependence was seen in the layers with higher Mn content. This can be explained by the metallic screening of the Mn ions, which prevents positron trapping at the hydrogenic states around Mn at high Mn content. At $T > 300$ K the annihilation parameters remain constant in all the layers.

Thus it can be concluded that the Ga vacancies are dominant positron traps in all the layers above room temperature, and their concentration can be estimated from the S and W parameters at 300 K using the conventional trapping model [13]. The Ga vacancy concentrations are presented in Fig. 4. It is clearly seen that the Ga vacancy concentration decreases with increasing Mn concentration from 2×10^{18} cm^{-3} in the undoped LT GaAs to 4×10^{16} cm^{-3} in the $Ga_{1-x}Mn_xAs$ layers with Mn content above 1%.

According to theoretical calculations [21], the electronic part of the formation energy of the acceptor-type Ga vacancy increases and of the donor-type As antisite decreases when the Fermi level approaches the valence band. In our experiments this thermodynamical trend is observed as the decrease of the Ga vacancy concentration and the increase of the As antisite concentration with increasing Mn content (Fig. 4). In $Ga_{1-x}Mn_xAs$ with high Mn content the Fermi level is very close to the valence band. The theory then predicts that the Ga vacancies should be neutral and the As antisites should be in a doubly positive charge state [21]. In this situation the difference of the formation energies of the two defects is about 2.5–3.5 eV [21]. Assuming that the defect concentrations in the LT-MBE grown layers are determined by the thermodynamical equilibrium, the difference of the formation energies can be determined from Fig. 4 as $E_F^{V_{Ga}} - E_F^{As_{Ga}} = kT \ln([As_{Ga}]/[V_{Ga}]) \simeq 200$–$400$ meV. This value is significantly smaller than that obtained from the theory, indicating that the absolute defect concentrations are determined by growth kinetics rather than

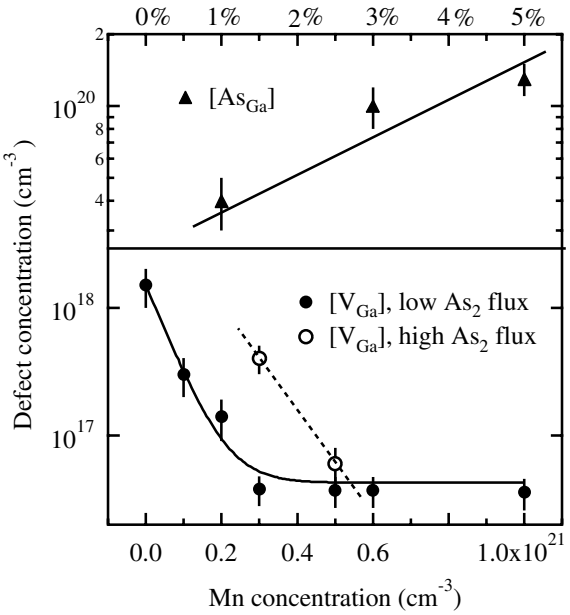

FIG. 4. The Ga vacancy and As antisite concentrations in the $Ga_{1-x}Mn_xAs$ layers as a function of the Mn concentration. The solid curve as well as the solid and dotted lines are drawn to guide the eye.

by thermodynamical equilibrium. This holds especially for the Ga vacancy concentration, which increases when the As_2 flux at growth is increased, the effect being stronger with lower Mn content.

The As antisite concentrations in the $Ga_{1-x}Mn_xAs$ layers are large enough to be significant for the compensation of the Mn acceptors and thus to affect the magnetic properties both through compensation and magnetic coupling [22,23]. They are, however, too low to explain all of the self-compensation of the material. In similar layers, the Mn interstitial concentration has been estimated to be around 15% of the total Mn concentration [24]. By adding the effect of these two types of defects together the total electrical compensation of the Mn doping can be explained.

The magnetic properties of the layers can be significantly improved by low temperature annealing due to the redistribution of Mn in the lattice [12,25,26]. Ga vacancies have been proposed to have an active role in the clustering of As antisites and substitutional Si in LT GaAs [6–10]. Their presence, especially at concentrations significantly higher than expected from the thermodynamical equilibrium, may also affect the Mn diffusion by the vacancy mechanism in the Ga sublattice, particularly since Ga vacancies are mobile at the typical growth and annealing temperatures around 250 °C [20].

In summary, we have used infrared absorption and positron annihilation spectroscopies to study the native Ga sublattice defects in LT-MBE grown $Ga_{1-x}Mn_xAs$ layers with Mn content ranging from 0% to 5%. We have shown that the concentrations of both As antisites (donors) and Ga vacancies (acceptors) vary as a function of the Mn content following thermodynamic trends, but the absolute concentrations are determined by the growth kinetics and stoichiometry. The As antisite concentrations ($\sim 10^{20}$ cm^{-3}) are significant for the hole compensation and magnetic properties. The presence of the Ga vacancies in the lattice may enhance the diffusion of Mn in the group III sublattice during the postgrowth annealing that improves the magnetic properties of the layers.

This work was supported by the Academy of Finland (SPIN project), by the Swedish Research Council (VR), and by the Swedish Foundation of Strategic Research (SSF). One of the authors (J. S.) acknowledges financial support from the Polish State Committee for Scientific Research (KBN) through Grants No. 2-P03B-05423 and No. PBZ-KBN-044/P03/2001.

*Electronic address: filip.tuomisto@hut.fi

[1] J. K. Furdyna, J. Appl. Phys. **64**, R29 (1988).
[2] H. Ohno, J. Magn. Magn. Mater. **200**, 110 (1999).
[3] T. Dietl *et al.*, Science **287**, 1019 (2000).
[4] T. Dietl, H. Ohno, and F. Matsukura, Phys. Rev. B **63**, 195205 (2001).
[5] T. Jungwirth *et al.*, Appl. Phys. Lett. **83**, 320 (2003).
[6] J. Gebauer *et al.*, Appl. Phys. Lett. **71**, 638 (1997).
[7] M. Luysberg *et al.*, J. Appl. Phys. **83**, 561 (1997).
[8] T. Laine *et al.*, J. Appl. Phys. **86**, 1888 (1999).
[9] J. Gebauer *et al.*, J. Appl. Phys. **87**, 8368 (2000).
[10] J. Gebauer *et al.*, Appl. Phys. Lett. **79**, 4313 (2001).
[11] F. Tuomisto *et al.*, Acta Phys. Pol. A **103**, 601 (2003).
[12] J. Sadowski and J. Z. Domagala, Phys. Rev. B **69**, 075206 (2004).
[13] K. Saarinen, P. Hautojärvi, and C. Corbel, in *Identification of Defects in Semiconductors*, edited by M. Stavola (Academic Press, New York, 1998), p. 209.
[14] P. Silverberg, G. Omling, and L. Samuelson, Appl. Phys. Lett. **52**, 1689 (1988).
[15] G. Vincent, D. Bois, and A. Chantre, J. Appl. Phys. **53**, 3643 (1982).
[16] S. K. Brierley and D. S. Lehr, Appl. Phys. Lett. **55**, 2426 (1989).
[17] M. Haiml *et al.*, Appl. Phys. Lett. **79**, 4313 (2001).
[18] K. Saarinen *et al.*, Phys. Rev. B **44**, 10 585 (1991).
[19] J. Gebauer *et al.*, Phys. Rev. B **60**, 1464 (1999).
[20] C. Corbel *et al.*, Phys. Rev. B **45**, 3386 (1992).
[21] J. E. Northrup and S. B. Zhang, Phys. Rev. B **47**, 6791 (1993).
[22] P. A. Korzhavyi *et al.*, Phys. Rev. Lett. **88**, 187202 (2002).
[23] S. Sanvito and N. A. Hill, Appl. Phys. Lett. **78**, 3493 (2001).
[24] K. M. Yu *et al.*, Phys. Rev. B **65**, 201303(R) (2002).
[25] K. W. Edmonds *et al.*, Phys. Rev. Lett. **92**, 037201 (2004).
[26] B. J. Kirby *et al.*, Phys. Rev. B **69**, 081307(R) (2004).